Psychological Medicine

cambridge.org/psm

Thalamic dysconnectivity in the psychosis risk syndrome and early illness schizophrenia

Susanna L. Fryer[1,2,*], Jamie M. Ferri[2,*], Brian J. Roach[2], Rachel L. Loewy[1], Barbara K. Stuart[1], Alan Anticevic[3,4], Judith M. Ford[1,2] and Daniel H. Mathalon[1,2]

[1]Department of Psychiatry, University of California, San Francisco, San Francisco, CA, USA; [2]San Francisco VA Healthcare System, San Francisco, CA, USA; [3]Department of Psychiatry, Yale School of Medicine, New Haven, CT, USA and [4]Department of Psychology, Yale University, New Haven, CT, USA

Abstract

Background. Schizophrenia (SZ) is associated with thalamic dysconnectivity. Compared to healthy controls (HCs), individuals with SZ have hyperconnectivity with sensory regions, and hypoconnectivity with cerebellar, thalamic, and prefrontal regions. Despite replication of this pattern in chronically ill individuals, less is known about when these abnormalities emerge in the illness course and if they are present prior to illness onset.

Methods. Resting-state functional magnetic resonance imaging data were collected from psychosis risk syndrome (PRS) youth ($n = 45$), early illness SZ (ESZ) ($n = 74$) patients, and HCs ($n = 85$). Age-adjusted functional connectivity, seeded from the thalamus, was compared among the groups.

Results. Significant effects of group were observed in left and right middle temporal regions, left and right superior temporal regions, left cerebellum, and bilateral thalamus. Compared to HCs, ESZ demonstrated hyperconnectivity to all temporal lobe regions and reduced connectivity with cerebellar, anterior cingulate, and thalamic regions. Compared to HCs, PRS demonstrated hyperconnectivity with the left and right middle temporal regions, and hypoconnectivity with the cerebellar and other thalamic regions. Compared to PRS participants, ESZ participants were hyperconnected to temporal regions, but did not differ from PRS in hypoconnectivity with cerebellar and thalamic regions. Thalamic dysconnectivity was unrelated to positive symptom severity in ESZ or PRS groups.

Conclusions. PRS individuals demonstrated an intermediate level of thalamic dysconnectivity, whereas ESZ showed a pattern consistent with prior observations in chronic samples. These cross-sectional findings suggest that thalamic dysconnectivity may occur prior to illness onset and become more pronounced in early illness stages.

Introduction

Disrupted connectivity across distributed neural networks has been proposed as a pathophysiological mechanism underlying schizophrenia (SZ) (Andreasen, 1999; Cannon, 2015; Friston, 1998; Stephan, Baldeweg, & Friston, 2006; Stephan, Friston, & Frith, 2009). These widespread abnormalities can be investigated using resting-state functional magnetic resonance imaging (fMRI)-based connectivity, which measures the temporal synchronization of low-frequency oscillations of the blood oxygen level-dependent (BOLD) signal between brain regions (Biswal, Yetkin, Haughton, & Hyde, 1995; Raichle, 2011).

While abnormalities have been observed across several functional networks in SZ, dysconnectivity within thalamo–striatal–cortico–cerebellar circuits has been widely replicated (e.g. Anticevic et al., 2014; Cheng et al., 2015; Damaraju et al., 2014; Klingner et al., 2014; Li et al., 2017; Woodward, Karbasforoushan, & Heckers, 2012). Converging evidence has substantiated findings of thalamic hypoconnectivity withprefrontal and cerebellar regions, as well as thalamic hyperconnectivity with sensory regions, suggesting thalamo–striatal–cortico–cerebellar dysconnectivity as a potential biomarker of SZ. Findings that are inconsistent with this pattern [e.g. (Guller, Tononi, & Postle, 2012; Wang, Rau, Li, Chen, & Yu, 2015)], may stem from heterogeneity in study methodologies and samples common in fMRI research. Further, aspects of thalamic dysconnectivity may relate to positive symptoms, with observations of positive correlations with the thalamus and middle temporal hyperconnectivity and negative correlations with cerebello–thalamic hypoconnectivity (Ferri et al., 2018).

While thalamic dysconnectivity is better characterized in chronic SZ, less is known regarding when these abnormalities emerge in the illness course. Neurodevelopmental models of SZ (e.g. Feinberg, 1982; Weinberger, 1987) suggest that abnormalities arise prior to illness onset, stemming from abnormal brain maturation including insufficient pruning of thalamic-sensory connections (Fair et al., 2010; Giraldo-Chica & Woodward, 2017). However, most investigations of thalamic dysconnectivity in SZ focused on adults with a chronic illness course (e.g.

Original Article

*Co-first authors.

Cite this article: Fryer SL, Ferri JM, Roach BJ, Loewy RL, Stuart BK, Anticevic A, Ford JM, Mathalon DH (2022). Thalamic dysconnectivity in the psychosis risk syndrome and early illness schizophrenia. *Psychological Medicine* **52**, 2767–2775. https://doi.org/10.1017/S0033291720004882

Received: 25 October 2019
Revised: 14 November 2020
Accepted: 26 November 2020
First published online: 15 March 2021

Key words:
connectivity; ultra-high risk; clinical high risk for psychosis; transition aged youth; first-episode schizophrenia

Author for correspondence:
Daniel H. Mathalon,
E-mail: daniel.mathalon@ucsf.edu

CAMBRIDGE UNIVERSITY PRESS

Anticevic et al., 2014; Cheng et al., 2015; Damaraju et al., 2014; Klingner et al., 2014; Li et al., 2017; Woodward et al., 2012). Woodward and Heckers (2016) report thalamic dysconnectivity early in the course of SZ (ESZ), with hypoconnectivity between the thalamus and cerebellum, and hyperconnectivity between the thalamus and somatosensory cortices in individuals <2 years from illness onset. Anticevic et al. (2015) report similar abnormalities in a large sample of individuals with psychosis risk syndrome (PRS), with dysconnectivity being more pronounced in those who subsequently developed a psychotic illness. Furthermore, when healthy control (HC) and PRS samples were considered together, there was a negative relationship between positive symptoms and thalamic hypoconnectivity.

These findings suggest that thalamic dysconnectivity patterns observed in chronic SZ may also be present in earlier illness stages. However, with so few studies of thalamic functional connectivity in ESZ and PRS, prior findings warrant replication, as well as the examination of ESZ and PRS samples within the same study. Accordingly, the current study examined whole-brain resting-state thalamic functional connectivity in a sample of 45 individuals meeting PRS criteria, 74 individuals with ESZ and 85 HCs. We also examined five *a priori* regions of interest (ROIs) that were functionally defined from group differences observed in the multisite North American Prodrome Longitudinal Study (NAPLS-2) cohort in a prior PRS study of thalamic connectivity (Anticevic et al., 2015). For both whole-brain and ROI-based analyses, we hypothesized that the PRS group would demonstrate increased thalamic connectivity with sensory regions and reduced thalamic connectivity with the cerebellum and prefrontal regions relative to HCs, and that these effects would be more pronounced in the ESZ group. We also examined the relationships between positive symptoms and thalamic dysconnectivity previously observed in chronic SZ (Ferri et al., 2018) and PRS (Anticevic et al., 2015) samples.

Methods

PRS participants ($n = 45$) were recruited from the University of California, San Francisco's (UCSF) Path program. PRS participants met Criteria of Psychosis-risk Syndromes (COPS) based on the structured interview for psychosis-risk syndromes (SIPS) (McGlashan, Walsh, & Woods, 2010; Miller et al., 2002, 2003), for at least one of three sub-syndromes: attenuated positive symptom state (APSS; $n = 43/45$), brief intermittent psychotic state (BIPS $n = 0/45$), and/or genetic risk and deterioration state (GRDS $n = 5/45$). Symptom severity in PRS patients was assessed using the scale of prodromal symptoms (SOPS).

ESZ patients ($n = 74$) within 5 years of illness onset (mean = 1.72 ± 1.35 years) were recruited from the Early Psychosis Clinic at UCSF and the community. Diagnosis of SZ or schizoaffective disorder was confirmed using the Structured Clinical Interview for DSM-IV-TR (SCID) (First, Spitzer, Gibbon, & Williams, 2002). The scale for the assessment of positive symptoms (SAPS; Andreasen, 1984) and the scale for the assessment of negative symptoms (SANS; Andreasen, 1989) were used to assess clinical symptom severity in ESZ. The majority of ESZ patients were prescribed antipsychotic medication ($n = 66/74$; 89.2%) while none of the PRS participants were ($n = 0/45$; 0%). After participating in neuroimaging, PRS participants were followed for 24 months or until they transitioned to psychosis. Six PRS individuals transitioned to a psychotic disorder [i.e. met the presence of psychotic symptom (POPS) criteria; Miller et al., 2003] while 21 were followed for the full 24-month follow-up period and did not transition to psychosis (with the remainder lost to follow-up).

HC participants ($n = 85$) recruited from the community were screened for Axis I disorders with the SCID-IV-TR (First et al., 2002), or for HC <16, the Kiddie-Schedule for Affective Disorders and Schizophrenia for school-age children-present and lifetime version (Kaufman et al., 1997).

Participants were 12–35 years old and were excluded for diagnostic and statistical manual of mental disorders (DSM-IV) past-year substance dependence (excepting nicotine), a history of head injury with loss of consciousness, central nervous system disorder, or, for HC participants, a first-degree relative with a psychotic illness. Written informed consent or assent was obtained from study participants under protocols approved by the Institutional Review Board at UCSF. This protocol complies with the ethical standards of national and international committees on human experimentation and with the Helsinki Declaration of 1975, as revised in 2008.

Data acquisition and processing

Resting fMRI data were acquired on a Siemens 3T TIM TRIO scanner at the UCSF Neuroimaging Center using a whole-brain echo-planar imaging (EPI) sequence (6 min): 180 functional images were acquired (32 axial slices, 3.5 mm slice thickness, 1.05 mm inter-slice gap, repetition time (TR) = 2 s, echo time (TE) = 29 ms, flip angle = 75°, field of view (FOV) = 24 cm). Participants were instructed to rest with their eyes open.

Image preprocessing was performed with Statistical Parametric Mapping (SPM8; http://www.fil.ion.ucl.ac.uk/spm/software/spm8/). Motion correction via affine registration realigned all images to the first image using INRIAlign (http://www.fil.ion.ucl.ac.uk/spm/ext/#INRIAlign). Images were slice-time corrected and the mean motion-corrected functional image was normalized to standard neuroanatomical space (Montreal Neurological Institute's MNI-EPI template; http://www.bic.mni.mcgill.ca), resulting in 3 mm^3 voxel dimensions. Data were spatially smoothed with a 6 mm full-width half-maximum Gaussian kernel. The artifact detection tools package (ART; http://www.nitrc.org/projects/artifact_detect/) identified outlying volumes based on global image intensity values ($Z > 3$) and head motion (>2 mm translational movement in the x, y, or z planes, or >0.02° rotation in yaw, pitch, or roll). ACompCor, a regression-based algorithm for denoising BOLD data, was applied (Behzadi, Restom, Liau, & Liu, 2007). ACompCor performs principal components analysis (PCA) on time-series data by deriving white matter and cerebrospinal fluid (CSF) noise regions from segmented high-resolution T1-weighted anatomical images co-registered to functional data. White matter noise regions were derived from FreeSurfer (http://surfer.nmr.mgh.harvard.edu/) segmentation, while CSF noise regions were derived from SPM8 segmentation. A binary union mask of noise ROIs was co-registered to the mean functional scan. Time-series data for the voxels in the noise masks were then subjected to PCA, and a number of noise components comprising weighted averages of white matter and CSF voxel time-series were identified using a bootstrap procedure (Behzadi et al., 2007).

The first-level GLM included the mean thalamic seed time-series and seven ART motion parameters, consisting of the temporal derivatives of the six motion parameters as well as a composite measure of total motion across translation and rotation. Regressors were also included for (i) data points identified by the ART toolbox as outliers

https://doi.org/10.1017/S0033291720004882 Published online by Cambridge University Press

and (ii) statistically significant ($p < 0.05$) principal noise components from the ACompCor denoising routine retained from each individual fMRI run.

Data analysis

To control for expected brain maturation across the age range studied and age differences between clinical groups, normal maturation effects were statistically removed from the functional connectivity data. We modeled normal aging effects in the HC group and calculated age-adjusted *Z*-scores for all subjects based on the HC group age-regression (Fryer et al., 2013a, 2013b, 2016; Mathalon, Pfefferbaum, Lim, Rosenbloom, & Sullivan, 2003; Pfefferbaum et al., 1992):

$$\frac{\text{Observed } r \text{ to } Z \text{ connectivity value} - \text{Predicted } r \text{ to } Z \text{ connectivity value}}{\text{Standard error of regression from HC age regression model}}.$$

Thus, a participant's age-adjusted *z*-score voxel-wise map reflects the deviation in functional connectivity, expressed in standard deviation units, from that expected for a healthy individual of the same age.

A seed-based connectivity analysis was conducted using the CONN toolbox (Whitfield-Gabrieli & Nieto-Castanon, 2012) (http://www.nitrc.org/projects/conn) with a bilateral seed of the whole thalamus, defined anatomically (Talairach Daemon atlas; Lancaster et al., 2000). The mean bilateral thalamic seed time-series vector was generated by averaging the time-series data across all seed voxels from the normalized functional images prior to smoothing. Voxel-wise correlation and anti-correlation (i.e. negative correlation) maps were generated for each subject, representing the Pearson's *r* correlation value between the seed time-series and every voxel in the brain. These *r* values were transformed to *Z*-scores via Fisher's transformation, resulting in voxel-wise thalamic functional connectivity *Z*-score maps for each participant.

Connectivity values were tested for significance between-groups in SPM8 on age-adjusted functional connectivity *Z*-score maps using a whole-brain false discovery rate (FDR) correction, $p < 0.01$. Mean connectivity values from FDR-corrected regions showing a significant main effect of *Group* (HC, ESZ, PRS) were extracted for all participants and followed-up with Tukey-Kramer honest significant difference (HSD) corrected *post-hoc* tests.

We also examined thalamic connectivity within five *a priori* ROIs generated from significant between-group differences in thalamic connectivity in an independent sample comparing HCs, PRS individuals who later converted to a psychotic disorder, and PRS individuals who did not (Anticevic et al., 2015). These ROIs included the left cerebellum, the right lateral PFC, the left sensory/motor cortex, the right sensory/motor cortex, and the anterior cingulate. Pairwise *t* testing followed-up differences in the thalamic connectivity between groups. Fisher *r*-to-*Z* transformed correlation coefficients were HC age-adjusted (*z*-scored) such that each subject's ROI mean reflects connectivity differences, in standardized units, from the expected connectivity for a healthy subject of the same age.

Scan head motion was compared between the groups via ANOVA by calculating the average motion displacement (Van Dijk, Sabuncu, & Buckner, 2012), defined as the root-mean-square (RMS) of the scan-to-scan change in *x*–*y*–*z* translation (in mm) or roll–pitch–yaw rotation (in degrees) parameters. The impact of differences in head motion between the groups was examined by re-running analyses with a covariate for the motion metrics (translational or rotational) that differed between groups. Antipsychotic medication effects within ESZ were examined by correlating chlorpromazine (CPZ) dosage equivalents (Danivas & Venkatasubramanian, 2013; Woods, 2003) with the extracted thalamic connectivity means from each ESZ patient within regions showing a significant Group effect. Non-parametric correlations (Spearman's ρ) were used due to the non-normality of the CPZ variable. Next, means for all clusters showing a significant main effect of *Group* were extracted and examined between PRS participants who converted to a psychotic disorder within 24 months of study entry ($n = 6$) *v.* non-converters ($n = 21$) who had been followed clinically for at least 24 months.

To examine clinical correlations, several families of tests were conducted guided by past studies in SZ and PRS groups. Our previous chronic SZ study (Ferri et al., 2018), reported thalamic dysconnectivity relationships with positive symptom severity driven by SAPS delusions and hallucinations global ratings. In PRS individuals, prior studies have shown the delusional thought (item P1: Unusual Thought Content; UTC) and suspiciousness (item P2) ratings to most strongly predict transition to psychosis, motivating a focus on these domains (Cannon et al., 2008; Perkins et al., 2015). In order to interrogate similar domains in ESZ and PRS groups, we included the SAPS persecutory ideas item in ESZ and the SOPS perceptual abnormalities/hallucinations item (item P4) in PRS. Thus, for all ROI clusters showing significant group effects, the ROIs were correlated with SAPS delusions, persecutory ideas, and hallucinations in ESZ, and SOPS UTC, suspiciousness, and SOPS perceptual abnormalities/hallucinations in PRS, with family-wise FDR correction ($p < 0.05$) applied to control type 1 error.

Lastly, in order to attempt to replicate correlations between connectivity and SOPS positive symptom totals in PRS (Anticevic et al., 2015), thalamic connectivity values were extracted from the exact ROI clusters reported by Anticevic et al. and summed to derive a separate hyperconnected and hypoconnected distributed ROI summary score. These two summary scores were then correlated with the SOPS positive symptom total score in the PRS sample (using a Bonferroni-adjusted α-level of 0.025). Mean age-adjusted (*z*-scored) connectivity values were extracted from the left cerebellum (peak MNI coordinate: $x = 39$, $y = -46$, $z = -47$) and the right medial temporal gyrus (MTG; $x = 63$, $y = -1$, $z = -23$) for each ESZ participant to test if the previously observed correlations in chronic SZ between thalamic dysconnectivity to these regions and SAPS global totals (Ferri et al., 2018) would replicate.

Results

Participant demographic and clinical data

The groups did not differ on gender ($p = 0.370$), handedness ($p = 0.145$), or average parental SES ($p = 0.133$). There were no significant group differences in rotational movement ($p > 0.29$), however there was a significant group effect ($p = 0.009$) of translational movement, with the HC group moving significantly less than the ESZ group ($p = 0.009$). There was a trend level group effect of age ($p = 0.07$), with the HC group being slightly older

https://doi.org/10.1017/S0033291720004882 Published online by Cambridge University Press

than the PRS group ($p = 0.05$). See Table 1 for group means and standard deviations for demographic and clinical variables.

Voxel-wise analyses

A main effect of *Group* was detected in eight age-adjusted and FDR-corrected regions. For all regions, the PRS group had mean thalamic connectivity values that numerically fell between those of HC and ESZ patients. Figure 1 and Table 2 depict the thalamic connectivity values and test statistics for pairwise *Group* follow-up tests for each cluster. Tukey HSD-corrected pairwise follow-up comparisons are reported below for each cluster.

(a) *Right middle/superior temporal gyrus* ($k = 189$). This cluster included the right middle and superior temporal gyri. Thalamic connectivity with this region was significantly greater in both ESZ and PRS relative to HC (p's < 0.001) and ESZ was significantly greater than PRS ($p = 0.023$).
(b) *Right middle temporal gyrus 1* ($k = 18$). This cluster contained voxels primarily from the right middle temporal gyrus with minor extension into the superior temporal gyrus. Thalamic connectivity to this region was significantly greater in ESZ and PRS relative to HC (p's < 0.001), however ESZ was not significantly different from PRS ($p = 1.00$).
(c) *Right middle temporal gyrus 2* ($k = 18$). This cluster contained voxels primarily from the right middle temporal gyrus with minor extension into the inferior temporal gyrus. Thalamic connectivity with this region was significantly greater in ESZ relative to HC ($p < 0.001$) and marginally greater relative to PRS ($p = 0.057$). PRS did not differ from HC ($p = 0.180$).
(d) *Left superior temporal gyrus* ($k = 37$). This cluster contained superior temporal gyrus. Thalamic connectivity with this region was significantly greater in ESZ compared to HC ($p < 0.001$) and PRS ($p = 0.028$), however PRS did not significantly differ from HC ($p = 0.189$).
(e) *Left middle temporal gyrus 1* ($k = 40$). This cluster primarily consisted of voxels from the middle temporal gyrus, but also extended into the middle occipital gyrus. Thalamic connectivity with this region was significantly greater in ESZ relative to both HC and PRS (p's < 0.001), however HC did not differ from PRS ($p = 0.878$).
(f) *Left middle temporal gyrus 2* ($k = 432$). This cluster primarily included the left middle temporal gyrus, extending into the left superior temporal gyrus. Thalamic connectivity with this region was significantly greater in ESZ relative to HC ($p < 0.001$) and marginally greater in ESZ compared to PRS ($p = 0.057$). HC did not differ from PRS ($p = 0.180$).
(g) *Bilateral thalamus* ($k = 592$). This cluster contained both left and right thalamus including the ventral lateral, medial dorsal, ventral anterior, lateral posterior, ventral posterior lateral, ventral posterior medial, and lateral dorsal nuclei. Thalamic connectivity with this region was significantly reduced in both ESZ and PRS relative to HC (p's < 0.001). ESZ was marginally less than PRS ($p = 0.088$).
(h) *Left cerebellum* ($k = 74$). This cluster was primarily in the posterior cerebellum, with extension into the anterior lobe. Thalamic connectivity with the left cerebellum was significantly reduced in both ESZ and PRS relative to HC (p's < 0.001), however ESZ was not significantly different from PRS ($p = 0.696$). Twenty (23%) of the 74 voxels in this cluster overlapped with the cerebellum ROI from Anticevic et al. (2015) study. There were no other overlapping voxels between this whole-brain analysis and the *a priori* ROI analyses described below.

ROI analyses

Cerebellum. Compared to HC, both PRS ($t(201) = -2.223$, $p = 0.027$) and ESZ ($t(201) = -2.755$, $p = 0.006$) demonstrated reduced connectivity between the cerebellum and the thalamus, consistent with our whole-brain findings.

Right lateral PFC. Compared to HC, thalamic connectivity with right lateral PFC was not significantly reduced in PRS ($t(201) = -1.166$, $p = 0.245$), or ESZ ($t(201) = -1.794$, $p = 0.074$, with a trend toward an effect in ESZ).

Left sensory/motor cortex. Compared to HC, thalamic connectivity to the left sensory/motor cortex was not significantly enhanced in PRS ($t(201) = 0.892$, $p = 0.373$), but was significantly enhanced in ESZ ($t(201) = 2.361$, $p = 0.019$).

Right sensory/motor cortex. Compared to HC, thalamic connectivity with the right sensory/motor cortex was not significantly enhanced in either PRS ($t(201) = 0.388$, $p = 0.669$) or ESZ ($t(201) = 1.541$, $p = 0.125$).

Anterior cingulate cortex (ACC). Thalamic connectivity with the ACC was marginally reduced in PRS compared to HC ($t(201) = -1.665$, $p = 0.097$) and significantly reduced in ESZ compared to HC ($t(201) = -3.27$, $p = 0.001$).

No significant differences were found between PRS and ESZ for any of the five ROIs (all p's > 0.260). Our results were all in the same direction as Anticevic et al. (2015) PRS study.

Motion artifact

Clusters showing a significant main effect of *Group* were extracted for all subjects, and analyses were repeated adding translational displacement as a covariate. All *Group* differences reported in the original analysis remained significant (all p's < 0.001). Corrected pairwise comparisons revealed the same pattern of significance, excepting the difference between PRS and ESZ for the left superior temporal gyrus changed from $p = 0.028$ to 0.053. Further, when dropping the nine ESZ subjects with the most translational movement from analysis, all comparisons of extracted cluster means remain significant (all p's < 0.001), with the same pattern of directionality.

Antipsychotic medication dosage in the ESZ group

Within our ESZ patient sample, CPZ equivalents did not covary with any of the regions showing the main effect of *Group* (Spearman's $\rho < |0.15|$; all p's >0.29).

Diagnosis within the ESZ group

Comparison of ESZ subgroups diagnosed with the schizoaffective disorder ($n = 23$) or SZ ($n = 51$), showed no significant differences in thalamic dysconnectivity between the diagnostic subgroups ($0.741 < p < 0.999$).

Psychosis transition within the PRS group

There were no significant differences between individuals who transitioned to a psychotic disorder ($n = 6$) and those who were clinically followed for 24 months and did not ($n = 21$) in any of the eight regions showing a main effect of group in thalamic

https://doi.org/10.1017/S0033291720004882 Published online by Cambridge University Press

Table 1. Demographic and clinical data for HC, PRS, and ESZ groups

	HC Mean ± S.D.	PRS Mean ± S.D.	ESZ Mean ± S.D.
N	85	45	74
Gender (% female)	40.00%	46.67%	33.78%
Age (years)	22.65 ± 20.17	20.34 ± 4.70	21.89 ± 4.22
Parental SES[a]	30.01 ± 14.00	33.89 ± 14.93	34.49 ± 15.84
Handedness (% right)	92.94%	86.67%	91.89%
Mean translational motion (mm)	0.059 ± 0.026	0.062 ± 0.031	0.073 ± 0.031
Mean rotational motion (°)	0.038 ± 0.019	0.043 + 0.022	0.042 ± 0.021
CPZ equivalents (mg)			276.11 ± 341.88
% Antipsychotic medication (typical, atypical, unknown, none)			3%; 81%; 5%; 11%
Psychotic disorder diagnosis (% SZ, schizoaffective)			69%; 31%
Total symptom ratings:			
SAPS global			16.74 ± 13.88
SANS global			37.93 ± 17.39
SOPS positive		9.33 ± 4.17	
SOPS negative		11.63 ± 5.94	
SOPS disorganized		5.44 ± 3.38	
SOPS general		8.68 ± 4.56	

[a]Socioeconomic status (SES) measured by the Hollingshead two-factor index (Hollingshead & Redlich, 1958). Higher Hollingshead scores indicate lower SES. All other assessment measures are scaled such that higher scores reflect greater levels of the measured variable.

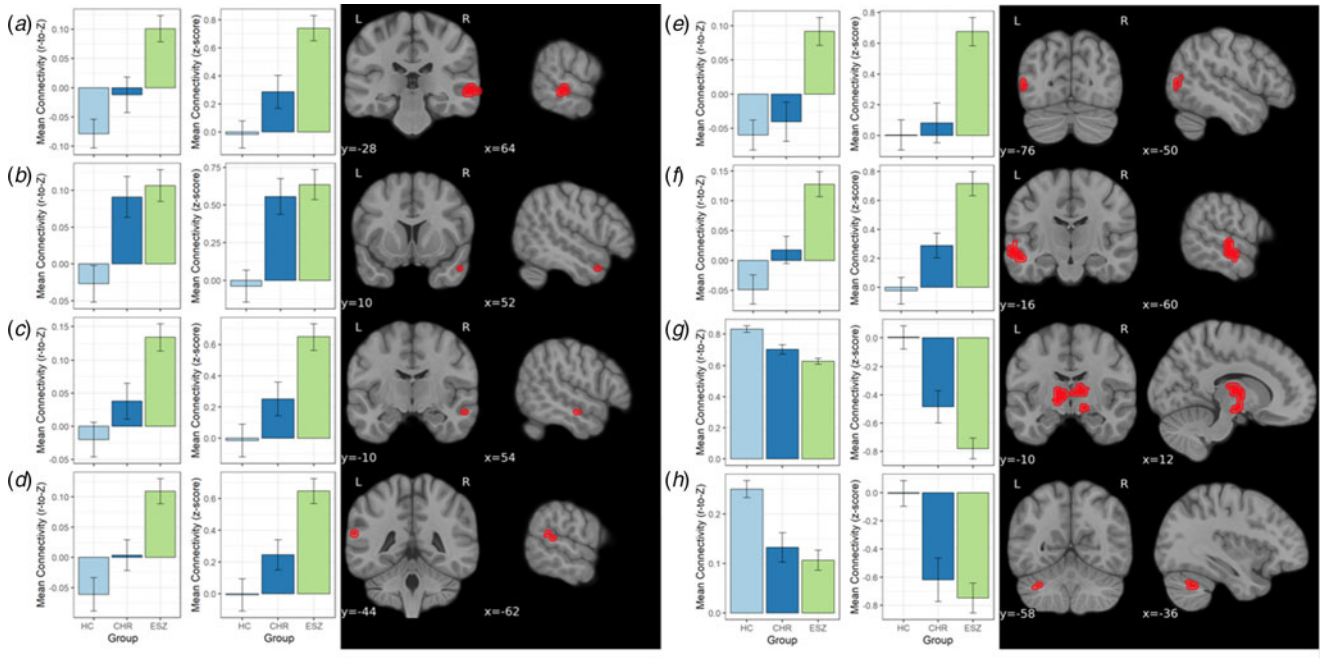

Fig. 1. Bar graphs display age-adjusted mean functional connectivity values by *Group* for each cluster showing a significant main effect of *Group* (FDR-corrected 0.010 height threshold). Regions correspond to cluster labels reported in the Results section and Table 2: (*a*) Right middle/superior temporal gyrus; (*b*) Right middle temporal gyrus 1; (*c*) Right middle temporal gyrus 2; (*d*) Left superior temporal gyrus; (*e*) Left middle temporal gyrus 1; (*f*) Left middle temporal gyrus 2; (*g*) Bilateral thalamus; (*h*) Left cerebellum.

https://doi.org/10.1017/S0033291720004882 Published online by Cambridge University Press

Table 2. Brain regions showing significant group differences in thalamic connectivity when comparing age-adjusted *z*-scores of HC ($n = 85$), PRS ($n = 74$), and ESZ ($n = 45$) groups

Cluster anatomy	Pairwise follow-up tests	Cluster size	Peak MNI coordinate (*x*, *y*, *z*)
(a) Right middle/superior temporal gyrus	HC < PRS, $p = 0.101$;	189	64, −28, −2
BA: 21/22	HC < ESZ, $p < 0.001$;		
	PRS < ESZ, $p = 0.023$		
(b) Right middle temporal gyrus 1	HC < PRS, $p < 0.001$;	18	52, 10, −30
BA: 21	HC < ESZ, $p < 0.001$;		
	PRS = ESZ, $p = 1.000$		
(c) Right middle temporal gyrus 2	HC = PRS, $p = 0.180$;	18	54, −10, −18
BA: 21	HC < ESZ, $p < 0.001$;		
	PRS < ESZ, $p = 0.057$		
(d) Left superior temporal gyrus	HC = PRS, $p = 0.189$;	37	−62, −44, 16
BA: 22	HC < ESZ, $p < 0.001$;		
	PRS < ESZ, $p = 0.028$		
(e) Left middle temporal gyrus 1	HC = PRS, $p < 0.878$;	41	−50, −76, 4
BA: 39/19	HC < ESZ, $p < 0.001$;		
	PRS < ESZ, $p < 0.001$		
(f) Left middle temporal gyrus 2	HC < PRS, $p = 0.053$;	432	−60, −16, −12
BA: 21/22	HC < ESZ, $p < 0.001$;		
	PRS < ESZ, $p < 0.024$		
(g) Bilateral thalamus	HC > PRS, $p < 0.001$;	592	12, −10, 6
	HC > ESZ, $p < 0.001$;		
	PRS = ESZ, $p = 0.088$		
(h) Left cerebellum	HC > PRS, $p < 0.001$;	74	−36, −58, −36
Posterior lobe	HC > ESZ, $p < 0.001$;		
	PRS = ESZ, $p = 0.696$		

connectivity (all p's > 0.20) or any of five regions from Anticevic et al. (2015) (all p's > 0.132).

Correlation of thalamic connectivity with clinical symptoms

No correlations survived adjustment for multiple comparisons within either ESZ or PRS groups for any of the regions examined.

Discussion

These results extend and replicate prior findings by showing thalamic dysconnectivity, in a single study, in both ESZ and PRS. Specifically, voxel-wise analyses demonstrated greater thalamic functional connectivity with middle and superior temporal regions, and reduced connectivity with cerebellar and thalamic regions in ESZ compared to HCs. ROI analyses revealed reduced thalamic connectivity with the cerebellum and the ACC and enhanced connectivity to the left sensory/motor cortex in ESZ compared to HCs. In the PRS group, voxelwise analyses indicated thalamic hyperconnectivity with some, but not all, middle temporal regions, and hypoconnectivity with cerebellar and thalamic regions compared to HCs. Similar to voxel-wise results, ROI analyses also revealed cerebellum hypoconnectivity in PRS patients that was equivalent to ESZ. Overall, these findings converge with the small literatures on ESZ (Woodward & Heckers, 2016) and PRS (Anticevic et al., 2015), and unlike previous studies, were obtained in one setting using identical methods, strengthening evidence that thalamic dysconnectivity patterns associated with chronic SZ are also present in earlier stages of the illness. The brain's intrinsic architecture can be organized into distributed, canonical networks, (Power et al., 2011; Yeo et al., 2011), with alterations of many of these well-described functional networks reported in SZ (e.g. Li et al., 2017). The thalamus is increasingly conceptualized as an integrative hub of functional connectivity, owing to its high degree of global connectivity to many discrete cortical regions; this challenges historical views of the thalamus as a 'passive' relay station, recasting the region instead as an actor that integrates information across disparate cortical networks (Hwang, Bertolero, Liu, & D'Esposito, 2017). Thus, the thalamic functional connectivity differences observed in our study likely have implications well-beyond discrete regional functioning, through extensive thalamic connectivity with other regions and networks.

Hyperconnectivity with temporal and sensory-motor areas and hypoconnectivity of cerebellar and ACC regions in ESZ patients compared to HCs largely replicate observations of enhanced sensory and reduced cerebellar and prefrontal connectivity in chronic

https://doi.org/10.1017/S0033291720004882 Published online by Cambridge University Press

patients (Anticevic et al., 2014; Ferri et al., 2018). A prior study in ESZ (Woodward & Heckers, 2016) defined six large cortical ROIs and the thalamus in HCs, chronic SZ and ESZ. Any portion of the thalamus showing group differences in connectivity to these six ROIs was then used as a functional thalamic ROI to seed a whole-brain connectivity analysis. Thus, discrepancies between the findings from Woodward and Heckers (2016) and our study may result from methodological differences that include seed definition. Despite these differences, both studies report enhanced thalamic-sensory region covariation in ESZ patients, which together provide evidence suggesting that thalamic dysconnectivity is not a result of the illness chronicity or prolonged medication use, but rather is observed early in the illness.

Thalamic dysconnectivity was also present in PRS, consistent with a previous thalamic seed-based study that reported hyperconnectivity to sensory regions and hypoconnectivity to cerebellar regions and the ACC in PRS (Anticevic et al., 2015). In the current study, as hypothesized, thalamic dysconnectivity observed in PRS individuals was more pronounced in ESZ, suggesting that thalamic connectivity abnormalities predate illness onset, but may worsen following illness onset (though this speculation warrants further study with a longitudinal design). In our sample, comparisons between PRS participants who transitioned to a psychotic disorder during a 24-month clinical follow-up period *v.* those who did not were underpowered because only six individuals converted to psychosis. In a larger sample ($n = 21$ converters) (Anticevic et al., 2015) individuals who subsequently transitioned to psychosis had a more exaggerated pattern of dysconnectivity at baseline, compared to those who did not. Further study is needed to establish thalamic dysconnectivity as a predictor of psychotic disorder transition. Nevertheless, the current findings suggest that thalamic dysconnectivity is present in PRS, representing a vulnerability marker that may intensify over the illness course. A NAPLS-2 study focused on 'cross-paradigm' connectivity to identify state-independent markers of psychosis risk across five paradigms, including resting state. The analysis revealed distributed hyperconnectivity in PRS that was associated with disorganization symptoms and predictive of time to psychosis transition, which suggests that increased cerebello–thalamo–cortical connectivity may be a trait marker of psychosis risk (Cao et al., 2018). The implication of distributed dysconnectivity in the cerebello–thalamo–cortical circuitry in PRS is also consistent with thalamic dysconnectivity observed in functional connectivity studies of PRS seeded fromtemporal (Colibazzi et al., 2017), cerebellar (Bernard, Orr, & Mittal, 2017), and striatal (Dandash et al., 2014) regions.

We did not observe significant correlations between thalamic dysconnectivity and positive symptom severity in ESZ or PRS groups. Previously observed correlations of thalamic dysconnectivity with SAPS global scores were obtained in a SZ patient sample with a longer illness duration (17.23 years on average), greater average age (38.73 years), and less variable (S.D. = 5.58) SAPS scores (see Table 1) (Ferri et al., 2018). However, the large chronic SZ sample size ($n = 183$) in our prior study provided >80% power to detect small magnitude (e.g. $|r| > 0.23$) correlations. While the ESZ sample in the current study is not small, there was half the power to detect equivalent magnitude correlations to those reported in (Ferri et al., 2018). Differences in the statistical power between the current study and (Anticevic et al., 2015) are greater; we were not powered to detect the small correlation ($r = -0.14$) between SOPS positive symptoms and mean hypoconnectivity observed in Anticevic et al.

We note several limitations of this study. First, there was insufficient clinical follow-up data to allow well-powered comparisons of PRS individuals who transitioned to a psychotic illness and those who did not. Next, we note that unlike some prior studies showing thalamo–striatal hypoconnectivity in both chronic SZ (Welsh, Chen, & Taylor, 2010) and PRS (Dandash et al., 2014) samples, we did not find group differences in connectivity between the thalamus and striatum. This may be a consequence of our voxel-wise analysis and corresponding type 1 error correction strategy which favors detection of larger regional effects over effects in smaller structures such as the striatum.

Another limitation is the antipsychotic medication use in the ESZ group. This limitation is mitigated by similar, albeit attenuated, findings of dysconnectivity in the PRS group, which was antipsychotic medication-free. However, this study was not designed to control for the effects of medication, and we cannot rule out the possibility of undetected medication effects confounding our results in the ESZ group. Widespread modulation of fMRI-based functional connectivity has been reported in association with antipsychotic medication use in first-episode patients with SZ (e.g. Lui et al., 2010), although these findings cannot distinguish between direct effects of antipsychotic medication and indirect effects mediated through the clinical improvements produced by medication. It remains an important future research direction to extend our work on thalamic functional connectivity to antipsychotic medication-free ESZ samples.

In conclusion, we replicate previous reports of reduced thalamic connectivity with cerebellar regions and increased connectivity with sensory regions in both individuals at high-risk for psychosis and early illness SZ, but in a single study. Our ROI analyses additionally replicate previous observations of increased connectivity with sensory-motor regions and decreased connectivity with the ACC in early illness SZ. Furthermore, our finding of similar but attenuated thalamic dysconnectivity in high-risk, medication-free PRS adds to a growing literature suggesting that patterns of thalamic connectivity that characterize chronic SZ may predate the onset of psychosis, motivating definitive examination of this question in a longitudinal dataset.

Acknowledgements. Research Supported by the National Institute of Mental Health (NIMH): MH076989 (DHM), MH58262, MH121900 (JMF); MH112189 (AA); Department of Veterans Affairs (VA): CX001028 (SLF), CX0004971 (JMF), Senior Research Career Scientist award to (JMF); NARSAD Independent Investigator Award (AA). Drs Fryer, Ford, and Mathalon are employees of the U.S. Government. The content is solely the responsibility of the authors and does not necessarily represent the views of the Department of Veterans Affairs.

Disclosures. Within the past three years, Dr Mathalon has received compensation as a consultant for Boehringer-Ingelheim, Syndisi, Cadent Therapeutics, and Recognify. . Within the past three years, Dr Anticevic has consulted, held equity and served as a scientific advisory board member for BlackThorn Therapeutics. Drs Ferri, Fryer, Ford, Lowey, Stuart and Mr Roach have no biomedical financial disclosures to declare.

Conflict of interest. None.

References

Andreasen, N. C. (1984). *The scale for the assessment of positive symptoms (SAPS)*. Iowa City, IA: University of Iowa.

Andreasen, N. C. (1999). A unitary model of schizophrenia: Bleuler's "fragmented phrene" as schizencephaly. *Archives of General Psychiatry*, *56*(9), 781–787. doi: 10.1001/archpsyc.56.9.781

https://doi.org/10.1017/S0033291720004882 Published online by Cambridge University Press

Andreasen, N. C. (1989). The scale for the assessment of negative symptoms (SANS): Conceptual and theoretical foundations. *The British Journal of Psychiatry Supplement*, *155*(7), 49–58. doi: 10.1192/S0007125000291496.

Anticevic, A., Cole, M. W., Repovs, G., Murray, J. D., Brumbaugh, M. S., Winkler, A. M., … Glahn, D. C. (2014). Characterizing thalamo-cortical disturbances in schizophrenia and bipolar illness. *Cerebral Cortex*, *24*(12), 3116–3130. doi: 10.1093/cercor/bht165.

Anticevic, A., Haut, K., Murray, J. D., Repovs, G., Yang, G. J., Diehl, C., … Cannon, T. D. (2015). Association of thalamic dysconnectivity and conversion to psychosis in youth and young adults at elevated clinical risk. *JAMA Psychiatry*, *72*(9), 882–891. doi: 10.1001/jamapsychiatry.2015.0566

Behzadi, Y., Restom, K., Liau, J., & Liu, T. T. (2007). A component based noise correction method (CompCor) for BOLD and perfusion based fMRI. *NeuroImage*, *37*(1), 90–101. doi: 10.1016/j.neuroimage.2007.04.042.

Bernard, J. A., Orr, J. M., & Mittal, V. A. (2017). Cerebello-thalamo-cortical networks predict positive symptom progression in individuals at ultra-high risk for psychosis. *NeuroImage: Clinical*, *14*, 622–628. doi: 10.1016/j.nicl.2017.03.001.

Biswal, B., Yetkin, F. Z., Haughton, V. M., & Hyde, J. S. (1995). Functional connectivity in the motor cortex of resting human brain using echo-planar MRI. *Magnetic Resonance in Medicine*, *34*(4), 537–541. doi: 10.1002/mrm.1910340409.

Cannon, T. D. (2015). Network dysconnectivity: A psychosis-triggering mechanism? *Biological Psychiatry*, *77*(11), 927–928. doi: 10.1016/j.biopsych.2015.03.019.

Cannon, T. D., Cadenhead, K., Cornblatt, B., Woods, S. W., Addington, J., Walker, E., … Heinssen, R. (2008). Prediction of psychosis in youth at high clinical risk: A multisite longitudinal study in North America. *Archives of General Psychiatry*, *65*(1), 28–37. doi: 10.1001/archgenpsychiatry.2007.3

Cao, H., Chén, O. Y., Chung, Y., Forsyth, J. K., McEwen, S. C., Gee, D. G., … Cannon, T. D. (2018). Cerebello-thalamo-cortical hyperconnectivity as a state-independent functional neural signature for psychosis prediction and characterization. *Nature Communications*, *9*(1), 3836. doi: 10.1038/s41467-018-06350-7.

Cheng, W., Palaniyappan, L., Li, M., Kendrick, K. M., Zhang, J., Luo, Q., … Feng, J. (2015). Voxel-based, brain-wide association study of aberrant functional connectivity in schizophrenia implicates thalamocortical circuitry. *NPJ Schizophrenia*, *1*, 15016. doi: 10.1038/npjschz.2015.16

Colibazzi, T., Yang, Z., Horga, G., Chao-Gan, Y., Corcoran, C. M., Klahr, K., … Peterson, B. S. (2017). Aberrant temporal connectivity in persons at clinical high risk for psychosis. *Biological Psychiatry: Cognitive Neuroscience and Neuroimaging*, *2*(8), 696–705. doi: 10.1016/j.bpsc.2016.12.008

Damaraju, E., Allen, E. A., Belger, A., Ford, J. M., McEwen, S., Mathalon, D. H., … Calhoun, V. D. (2014). Dynamic functional connectivity analysis reveals transient states of dysconnectivity in schizophrenia. *NeuroImage: Clinical*, *5*, 298–308. doi: 10.1016/j.nicl.2014.07.003

Dandash, O., Fornito, A., Lee, J., Keefe, R. S., Chee, M. W., Adcock, R. A., … Harrison, B. J. (2014). Altered striatal functional connectivity in subjects with an at-risk mental state for psychosis. *Schizophrenia Bulletin*, *40*(4), 904–913. doi: 10.1093/schbul/sbt093

Danivas, V., & Venkatasubramanian, G. (2013). Current perspectives on chlorpromazine equivalents: Comparing apples and oranges!. *Indian Journal of Psychiatry*, *55*(2), 207–208. doi: 10.4103/0019-5545.111475.

Fair, D. A., Bathula, D., Mills, K. L., Dias, T. G., Blythe, M. S., Zhang, D., … Nagel, B. J. (2010). Maturing thalamocortical functional connectivity across development. *Frontiers in Systems Neuroscience*, *4*, 10. doi: 10.3389/fnsys.2010.00010

Feinberg, I. (1982). Schizophrenia: Caused by a fault in programmed synaptic elimination during adolescence? *Journal of Psychiatric Research*, *17*(4), 319–334. doi: 10.1016/0022-3956(82)90038-3.

Ferri, J., Ford, J. M., Roach, B. J., Turner, J. A., van Erp, T. G., Voyvodic, J., … Mathalon, D. H. (2018). Resting-state thalamic dysconnectivity in schizophrenia and relationships with symptoms. *Psychological Medicine*, *48*(15), 2492–2499. doi: 10.1017/S003329171800003X

First, M. B., Spitzer, R. L., Gibbon, M., & Williams, J. B. (2002). *Structured clinical interview for DSM-IV-TR axis I disorders, research version, patient edition*. New York, NY: SCID-I/P.

Friston, K. J. (1998). The disconnection hypothesis. *Schizophrenia Research*, *30*(2), 115–125. doi: 10.1016/s0920-9964(97)00140-0.

Fryer, S. L., Jorgensen, K. W., Yetter, E. J., Daurignac, E. C., Watson, T. D., Shanbhag, H., … Mathalon, D. H. (2013b). Differential brain response to alcohol cue distractors across stages of alcohol dependence. *Biological Psychology*, *92*(2), 282–291. doi: 10.1016/j.biopsycho.2012.10.004

Fryer, S. L., Roach, B. J., Wiley, K., Loewy, R. L., Ford, J. M., & Mathalon, D. H. (2016). Reduced amplitude of low-frequency brain oscillations in the psychosis risk syndrome and early illness schizophrenia. *Neuropsychopharmacology: Official Publication of the American College of Neuropsychopharmacology*, *41*(9), 2388–2398. doi: 10.1038/npp.2016.51

Fryer, S. L., Woods, S. W., Kiehl, K. A., Calhoun, V. D., Pearlson, G. D., Roach, B. J., … Mathalon, D. H. (2013a). Deficient suppression of default mode regions during working memory in individuals with early psychosis and at clinical high-risk for psychosis. *Frontiers in Psychiatry*, *4*, 92. doi: 10.3389/fpsyt.2013.00092

Giraldo-Chica, M., & Woodward, N. D. (2017). Review of thalamocortical resting-state fMRI studies in schizophrenia. *Schizophrenia Research*, *180*, 58–63. doi: 10.1016/j.schres.2016.08.005

Guller, Y., Tononi, G., & Postle, B. R. (2012). Conserved functional connectivity but impaired effective connectivity of thalamocortical circuitry in schizophrenia. *Brain Connectivity*, *2*(6), 311–319. doi: 10.1089/brain.2012.0100

Hollingshead, A. B., & Redlich, F. C. (1958). *Social class and mental illness: Community study*. New York: John Wiley & Sons Inc. doi:10.1037/10645-000.

Hwang, K., Bertolero, M. A., Liu, W. B., & D'Esposito, M. (2017). The human thalamus is an integrative hub for functional brain networks. *The Journal of Neuroscience: The Official Journal of the Society for Neuroscience*, *37*(23), 5594–5607. doi: 10.1523/JNEUROSCI.0067-17.2017

Kaufman, J., Birmaher, B., Brent, D., Rao, U., Flynn, C., Moreci, P., … Ryan, N. (1997). Schedule for affective disorders and schizophrenia for school-age children-present and lifetime version (K-SADS-PL): Initial reliability and validity data. *Journal of the American Academy of Child and Adolescent Psychiatry*, *36*(7), 980–988. doi: 10.1097/00004583-199707000-00021.

Klingner, C. M., Langbein, K., Dietzek, M., Smesny, S., Witte, O. W., Sauer, H., & Nenadic, I. (2014). Thalamocortical connectivity during resting state in schizophrenia. *European Archives of Psychiatry and Clinical Neuroscience*, *264*(2), 111–119. doi: 10.1007/s00406-013-0417-0

Lancaster, J. L., Woldorff, M. G., Parsons, L. M., Liotti, M., Freitas, C. S., Rainey, L., … Fox, P. T. (2000). Automated Talairach atlas labels for functional brain mapping. *Human Brain Mapping*, *10*(3), 120–131. doi: 10.1002/1097-0193(200007)10:3 < 120::aid-hbm30>3.0.co;2-8

Li, T., Wang, Q., Zhang, J., Rolls, E. T., Yang, W., Palaniyappan, L., … Feng, J. (2017). Brain-wide analysis of functional connectivity in first-episode and chronic stages of schizophrenia. *Schizophrenia Bulletin*, *43*(2), 436–448. doi: 10.1093/schbul/sbw099

Lui, S., Li, T., Deng, W., Jiang, L., Wu, Q., Tang, H., … Gong, Q. (2010). Short-term effects of antipsychotic treatment on cerebral function in drug-naive first-episode schizophrenia revealed by "resting state" functional magnetic resonance imaging. *Archives of General Psychiatry*, *67*(8), 783–792. doi: 10.1001/archgenpsychiatry.2010.84

Mathalon, D. H., Pfefferbaum, A., Lim, K. O., Rosenbloom, M. J., & Sullivan, E. V. (2003). Compounded brain volume deficits in schizophrenia-alcoholism comorbidity. *Archives of General Psychiatry*, *60*(3), 245–252. doi: 10.1001/archpsyc.60.3.245

McGlashan, T., Walsh, B., & Woods, S. (2010). *The psychosis-risk syndrome: Handbook for diagnosis and follow-up*. New York, NY: Oxford University Press.

Miller, T. J., McGlashan, T. H., Rosen, J. L., Cadenhead, K., Cannon, T., Ventura, J., … Woods, S. W. (2003). Prodromal assessment with the structured interview for prodromal syndromes and the scale of prodromal symptoms: Predictive validity, interrater reliability, and training to reliability. *Schizophrenia Bulletin*, *29*(4), 703–715. doi: 10.1093/oxfordjournals.schbul.a007040

Miller, T. J., McGlashan, T. H., Rosen, J. L., Somjee, L., Markovich, P. J., Stein, K., & Woods, S. W. (2002). Prospective diagnosis of the initial prodrome for schizophrenia based on the Structured Interview for prodromal syndromes: Preliminary evidence of interrater reliability and predictive validity.

The American Journal of Psychiatry, *159*(5), 863–865. doi: 10.1176/appi.ajp.159.5.863

Perkins, D. O., Jeffries, C. D., Cornblatt, B. A., Woods, S. W., Addington, J., Bearden, C. E., … McGlashan, T. H. (2015). Severity of thought disorder predicts psychosis in persons at clinical high-risk. *Schizophrenia Research*, *169*(1–3), 169–177. doi: 10.1016/j.schres.2015.09.008

Pfefferbaum, A., Lim, K. O., Zipursky, R. B., Mathalon, D. H., Rosenbloom, M. J., Lane, B., … Sullivan, E. V. (1992). Brain gray and white matter volume loss accelerates with aging in chronic alcoholics: A quantitative MRI study. *Alcoholism, Clinical and Experimental Research*, *16*(6), 1078–1089. doi: 10.1111/j.1530-0277.1992.tb00702.x

Power, J. D., Cohen, A. L., Nelson, S. M., Wig, G. S., Barnes, K. A., Church, J. A., … Petersen, S. E. (2011). Functional network organization of the human brain. *Neuron*, *72*(4), 665–678. doi: 10.1016/j.neuron.2011.09.006

Raichle, M. E. (2011). The restless brain. *Brain Connectivity*, *1*(1), 3–12. doi: 10.1089/brain.2011.0019

Stephan, K. E., Baldeweg, T., & Friston, K. J. (2006). Synaptic plasticity and disconnection in schizophrenia. *Biological Psychiatry*, *59*(10), 929–939. doi: 10.1016/j.biopsych.2005.10.005

Stephan, K. E., Friston, K. J., & Frith, C. D. (2009). Disconnection in schizophrenia: From abnormal synaptic plasticity to failures of self-monitoring. *Schizophrenia Bulletin*, *35*(3), 509–527. doi: 10.1093/schbul/sbn176

Van Dijk, K. R., Sabuncu, M. R., & Buckner, R. L. (2012). The influence of head motion on intrinsic functional connectivity MRI. *NeuroImage*, *59*(1), 431–438. doi: 10.1016/j.neuroimage.2011.07.044

Wang, H. L., Rau, C. L., Li, Y. M., Chen, Y. P., & Yu, R. (2015). Disrupted thalamic resting-state functional networks in schizophrenia. *Frontiers in Behavioral Neuroscience*, *9*, 45. doi: 10.3389/fnbeh.2015.00045

Weinberger, D. R. (1987). Implications of normal brain development for the pathogenesis of schizophrenia. *Archives of General Psychiatry*, *44*(7), 660–669. doi: 10.1001/archpsyc.1987.01800190080012

Welsh, R. C., Chen, A. C., & Taylor, S. F. (2010). Low-frequency BOLD fluctuations demonstrate altered thalamocortical connectivity in schizophrenia. *Schizophrenia Bulletin*, *36*(4), 713–722. doi: 10.1093/schbul/sbn145

Whitfield-Gabrieli, S., & Nieto-Castanon, A. (2012). Conn: A functional connectivity toolbox for correlated and anticorrelated brain networks. *Brain Connectivity*, *2*(3), 125–141. doi: 10.1089/brain.2012.0073

Woods, S. W. (2003). Chlorpromazine equivalent doses for the newer atypical antipsychotics. *The Journal of Clinical Psychiatry*, *64*(6), 663–667. doi: 10.4088/jcp.v64n0607

Woodward, N. D., & Heckers, S. (2016). Mapping thalamocortical functional connectivity in chronic and early stages of psychotic disorders. *Biological Psychiatry*, *79*(12), 1016–1025. doi:10.1016/j.biopsych.2015.06.026.

Woodward, N. D., Karbasforoushan, H., & Heckers, S. (2012). Thalamocortical dysconnectivity in schizophrenia. *The American Journal of Psychiatry*, *169*(10), 1092–1099. doi: 10.1176/appi.ajp.2012.12010056

Yeo, B. T., Krienen, F. M., Sepulcre, J., Sabuncu, M. R., Lashkari, D., Hollinshead, M., … Buckner, R. L. (2011). The organization of the human cerebral cortex estimated by intrinsic functional connectivity. *Journal of Neurophysiology*, *106*(3), 1125–1165. doi: 10.1152/jn.00338.2011